



جامعة مصر للمعلوماتية
EGYPT UNIVERSITY
OF INFORMATICS

Dense plasma focus (DPF) and its applications

By

Mohamed I. Ismail

College of Engineering

Egypt University of Informatics

Outline

- Introduction to dense plasma focus devices.
- (KSU-DPF) device.
- Characterization of the device.
- Applications
 - Radiography and explosive detection

Dense plasma focus (DPF)

- DPF is a coaxial plasma accelerator that generates, accelerates and pinches a plasma by self-generated magnetic forces.
- DPF is a rich source of the following energetic radiations
 - Fast electrons (0.01 -1MeV)
 - Fast ions (0.01-100 MeV)
 - Soft (0.1-10 keV) and hard X rays (10-1000 keV)
 - Monoenergetic fusion neutrons
(2.45 MeV for D-D reactions or 14.1 MeV for D-T reactions).
- Independently discovered in the early 60s by Mather in the USA and Filippov in the former Soviet Union.

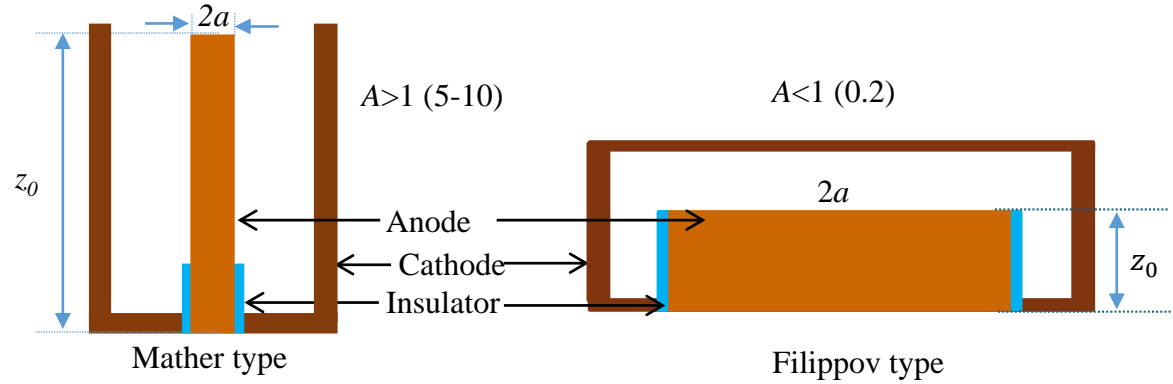
DPF Applications

- Nuclear Fusion energy source (not yet)
- Fast Neutron Activation Analysis
- Neutron Radiography
- X-ray radiography (hard x-ray)
- Lithography
- Material Science (deposition, modification, implantation)

Different configurations

Anode aspect ratio

$$(A) = \frac{z_0}{2a}$$



Different scales

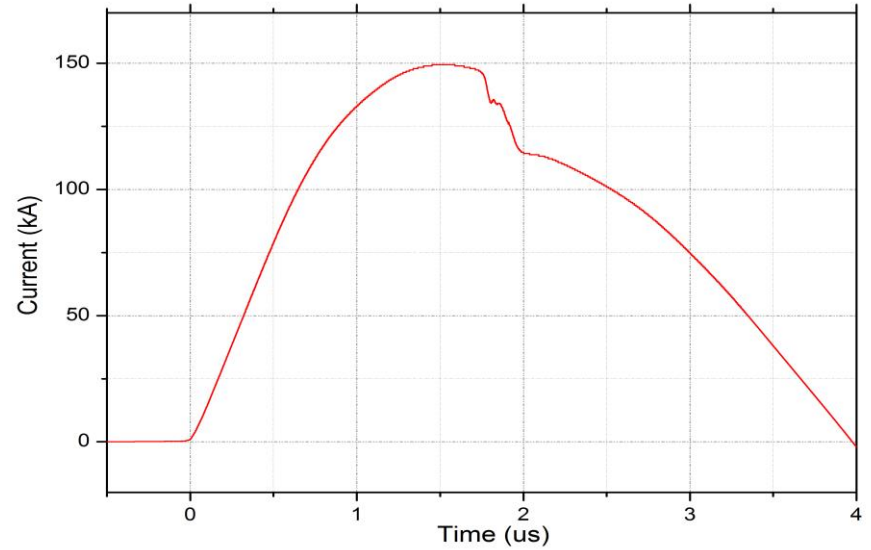
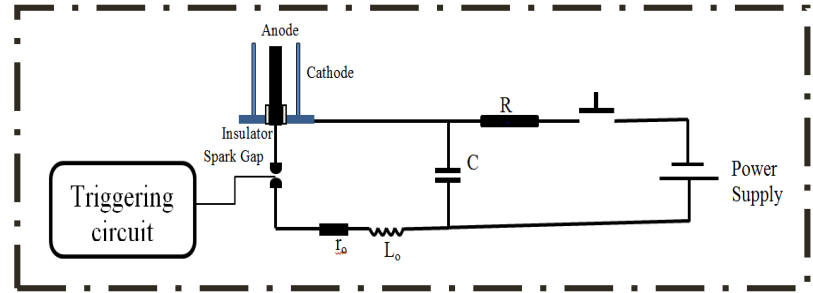
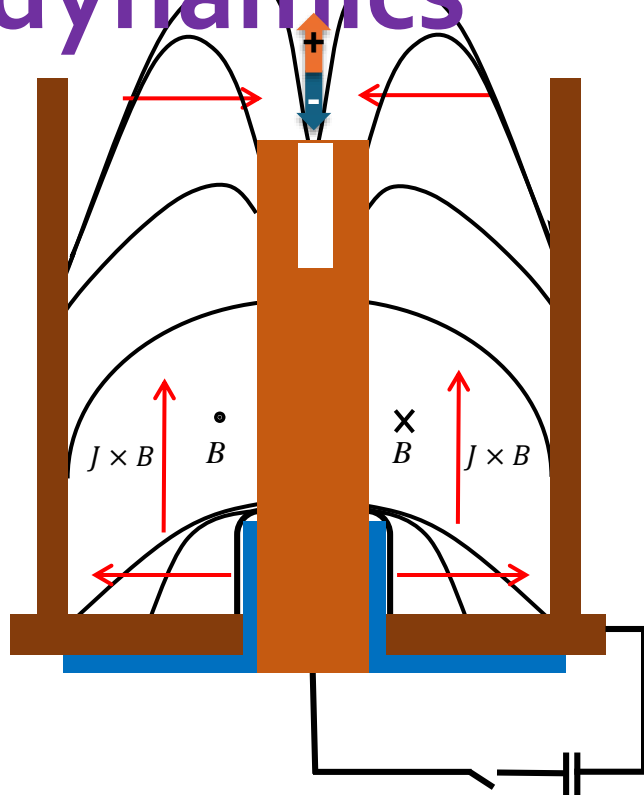


FMPF-1
(230 J)

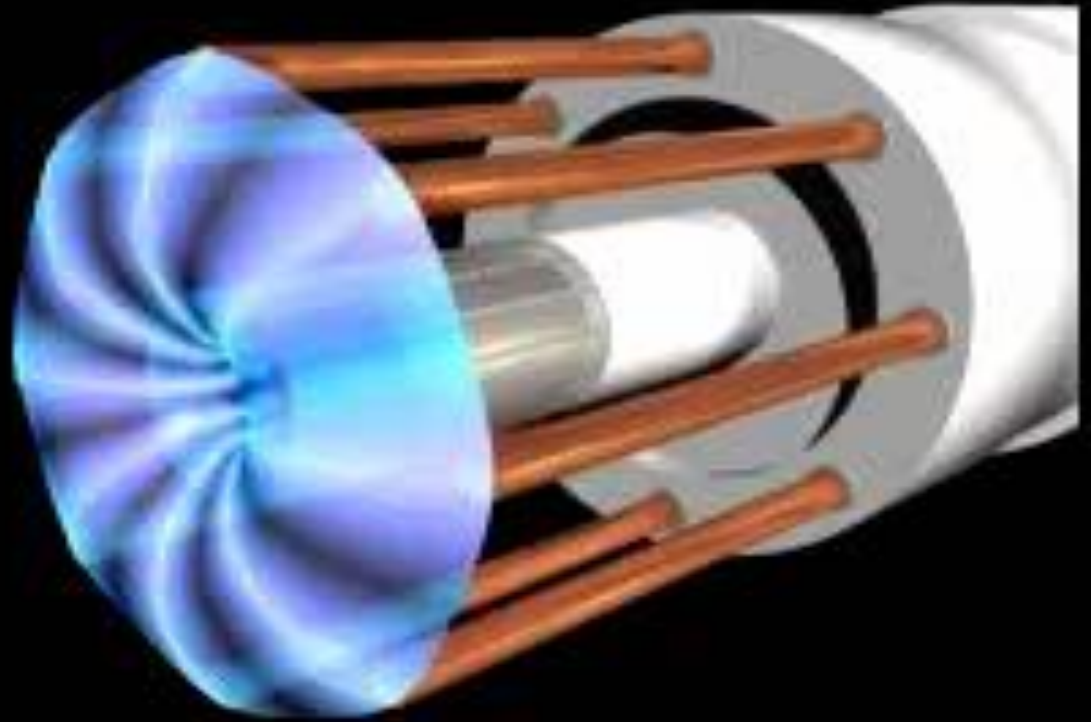


PF-1000
(1064 kJ)

DPF dynamics



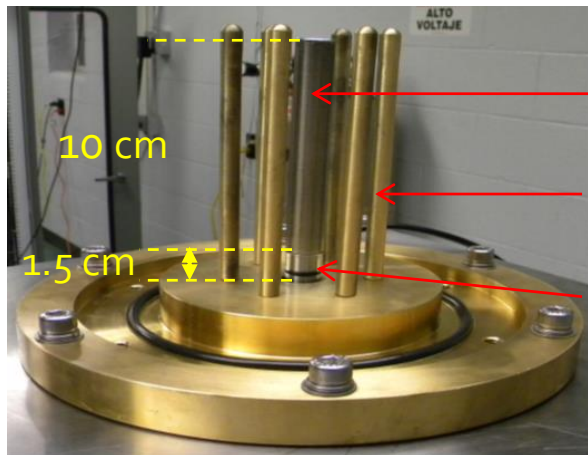
<http://lawrencevilleplasmaphysics.com/>



Outline

- Introduction to dense plasma focus, construction and dynamics.
- KSU-DPF specifications and characterization.
- X-ray emission characteristics of the KSU-DPF.
- Introduction to explosive detection methods.
- Signature- based radiation scanning (SBRS).
- Experimental work for explosive detection.
- Simulation.
- Conclusion.

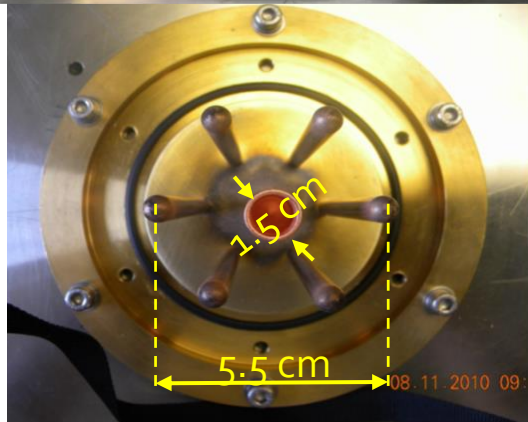
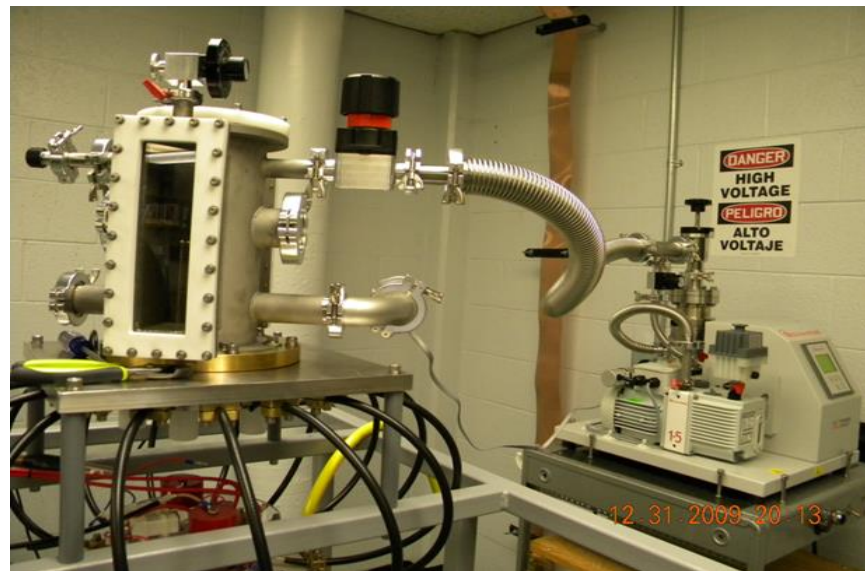
KSU-DPF



Anode

Cathode

Insulator



Different anode shapes & materials

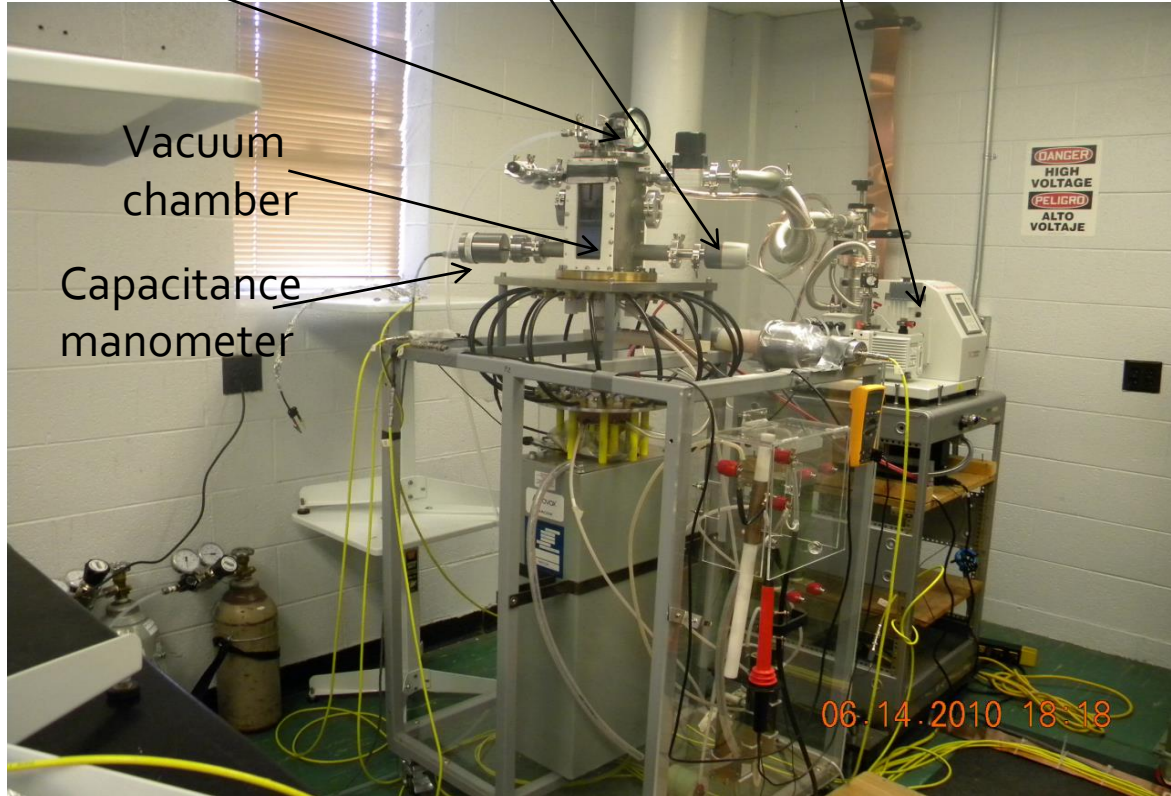
Mechanical
Pressure gauge

Wide range
Pressure gauge

Pumping
Station

Vacuum
chamber

Capacitance
manometer



Diagnostic tools



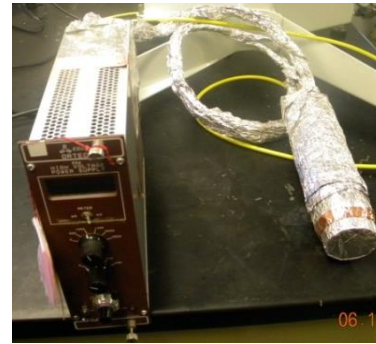
Rogowski coil



Voltage probe
Northstar HV5 80 MHz



Four channels
PIN diode
BPX65



BC-418 (2x1 in) plastic
scintillator, HAMAMATSU
PMT, model H7195.



Canberra (3x3 in) NaI(Tl)
scintillator, 3M3/3-X



Bubble
detector



⁶Lil scintillator



³He detector



Faraday cups
(SMA female connectors)



7000 series Tektronix DPO
Oscilloscope

KSU Electrical parameters

Parameter	Value
C_0	12.5 μF
$V_{max.}$	40 kV
E	Up to 10 kJ
I_{max}	150: 200 kA
L_0	91 \pm 2 nH
r_0	13 \pm 3 m Ω

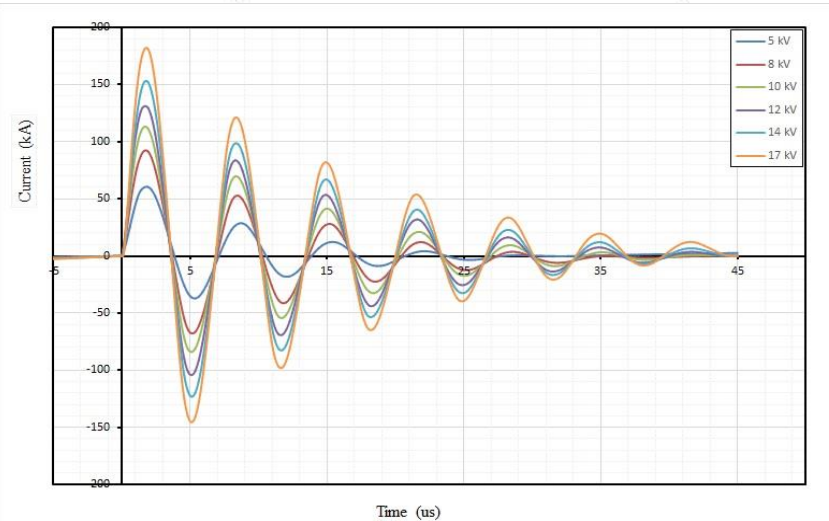
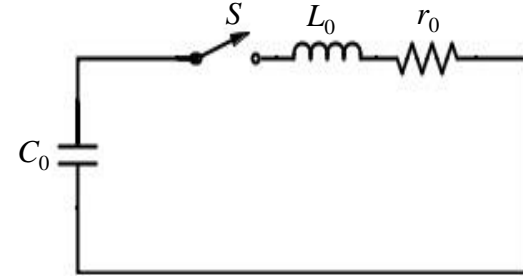
$$I_1(kA) = \frac{\pi C_0 V_0 (1 + k)}{T}$$

$$r_0 = \frac{2}{\pi} (\ln k) \left(\frac{L_0}{C_0} \right)$$

$$L_0 = \frac{T^2}{4\pi^2 C_0}$$

$$k = \frac{1}{n-1} \left(\frac{V_2}{V_1} + \frac{V_3}{V_2} + \dots + \frac{V_n}{V_{n-1}} \right)$$

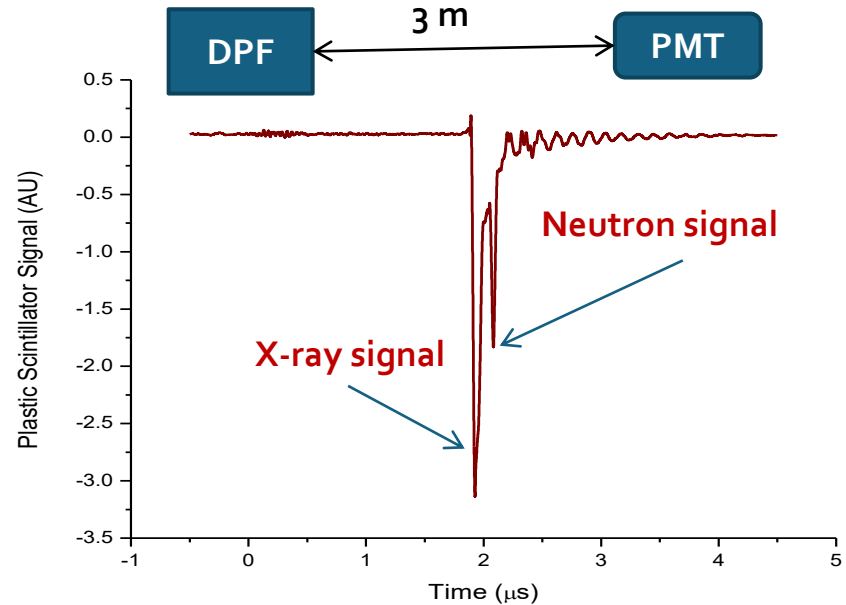
Average reversal ratio



Time of Flight

- (TOF) technique is used to give information on the time-resolved neutron energy.
- Scintillation-photomultiplier system to register the time resolved hard x-ray and neutron pulses.
- BC-418 plastic scintillator optically connected to HAMAMATSU H7195 Photomultiplier (PMT)

KSU-DPF



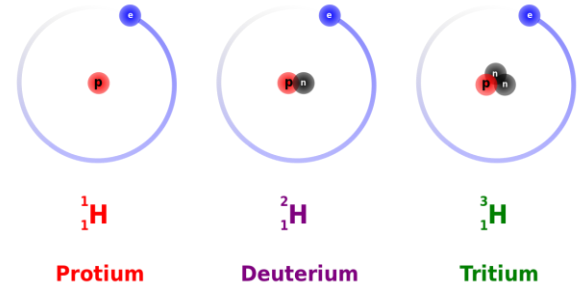
$$\Delta t = 138.74 \text{ ns}$$

$$E_n = 2.45 \text{ MeV}$$

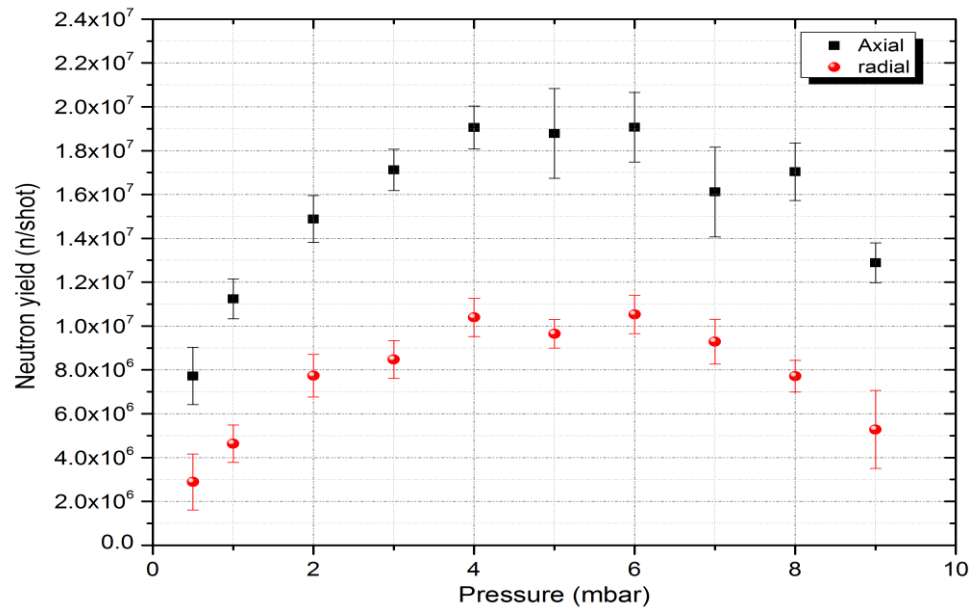
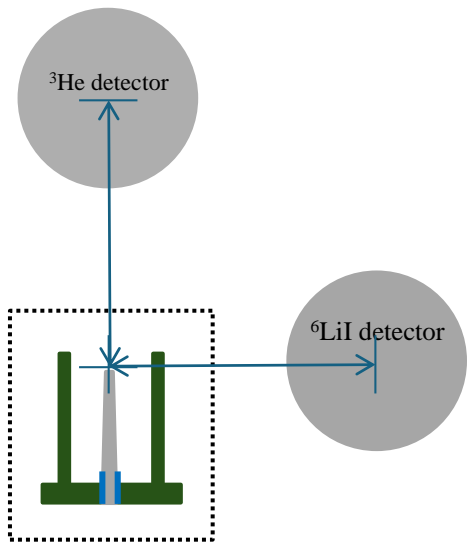
Neutron Yield

□ Neutron production

- Thermonuclear Reaction.



- Beam-Target Reaction. (2-11.3 MeV)



X-ray production

- **X-ray emission processes**

- 1- Bremsstrahlung (Free-Free) Radiation.**

Charged particle is accelerated or retarded. Electron accelerated in the coulomb fields of ions. (spectrum)

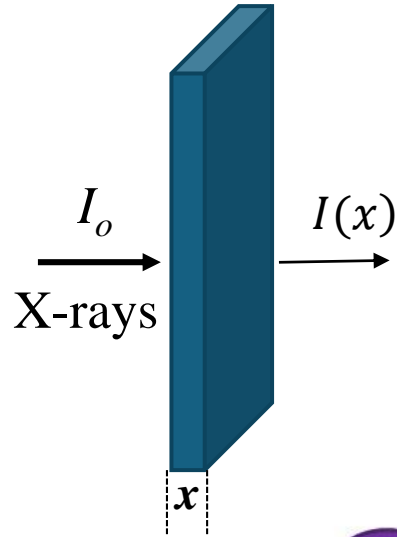
- 2- Recombination (Free-Bound) Radiation**

Free electron captured into a bound state of an ion. Photons emitted with the binding and initial electron kinetic energy (spectrum).

- 3- Line (Bound-Bound transition) Radiation**

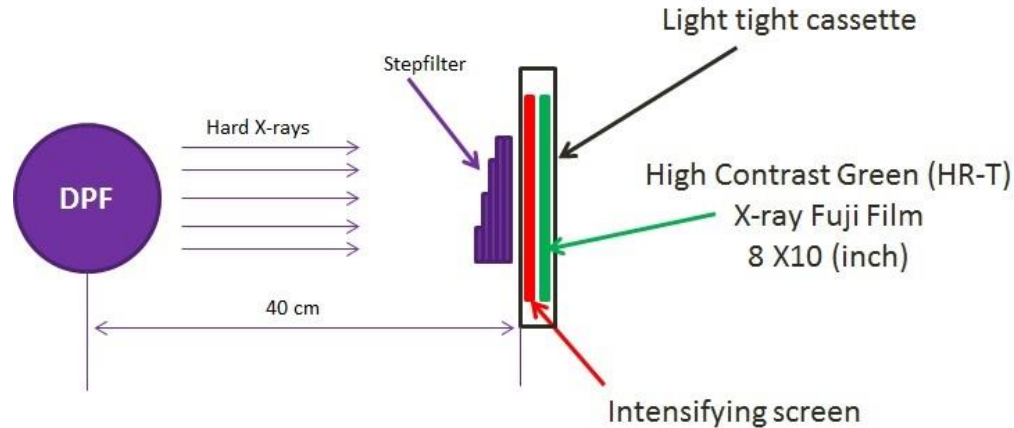
Electronic transition between the discrete or bound energy levels in atoms, (discrete packets of energy, or "lines", characteristic of the atom/ion)

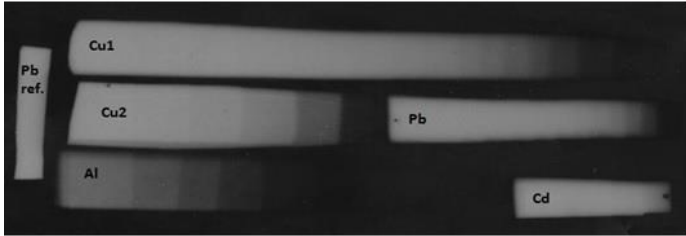
Average effective energy measurements



$$\frac{I(x)}{I_0} = e^{-\mu^* x}$$

$\mu^* = \mu(E^*)$: Linear attenuation coefficient at the average effective energy





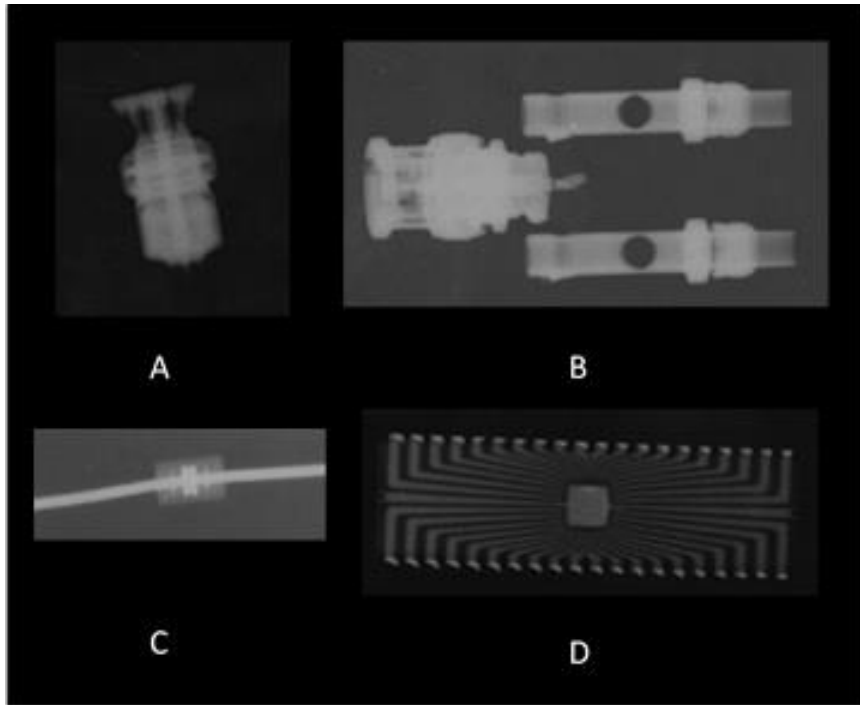
Material	Densit γ	μ^*	E^*
Cu1	8.96	14.98 ± 1.82	60 ± 3
Cu2	8.96	17.87 ± 2.34	56 ± 3
Al	2.7	0.79 ± 0.16	61 ± 10
Pb	11.34	60.51 ± 8.77	59 ± 4
Average			59 ± 3

← Different step filters used and its radiography

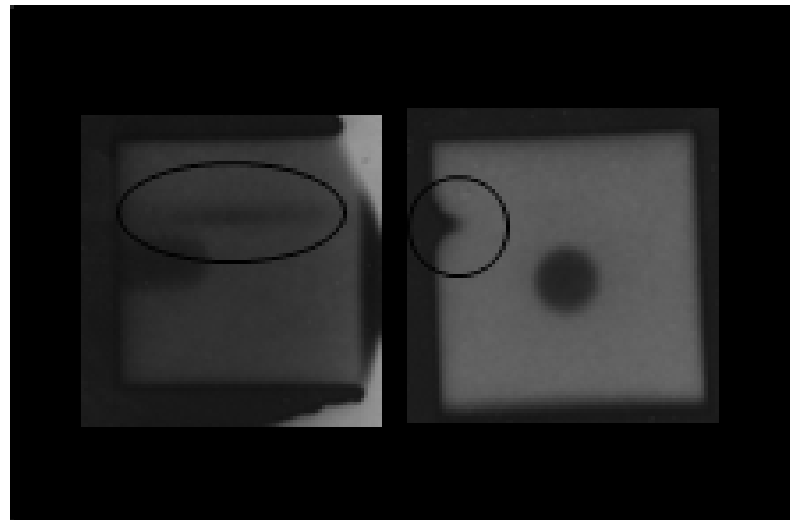


↑ X-RITE 301 densitometer used to measure the optical density (a), calibrated transmission set (b).

Radiography using KSU-DPF



A- BN connector, B- BNC male to dual binding post adapter, C- Resistor and D- IC.



An aluminum phantom (1" cube) has a crack and a hole in one side.

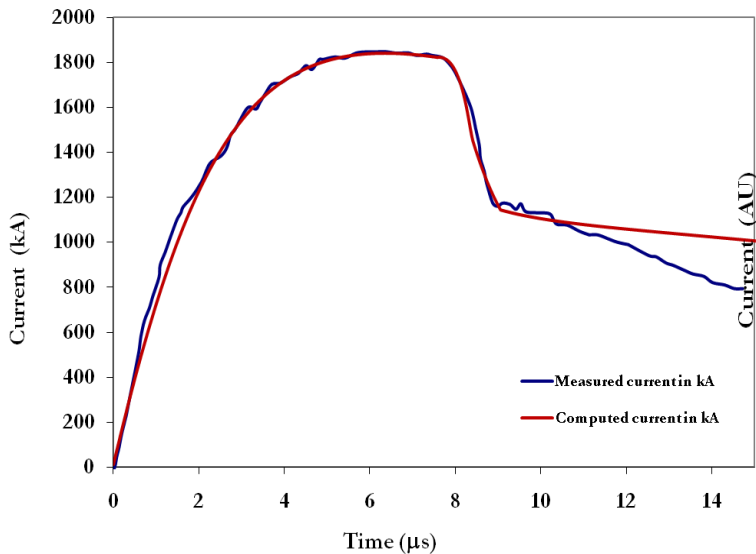
Lee model and high inductance devices

- Lee model couples electrical circuit with the plasma focus dynamics, thermodynamics and radiation.
- It computes SXR, neutron yield, pinch current, pinch time..etc.
- A computed current trace is fitted to a typical measured signal by adjusting what is called mass and current factors in both axial and radial phase.
- Developed in 1985 in two phases then upgraded in 2000 to 5-phases.

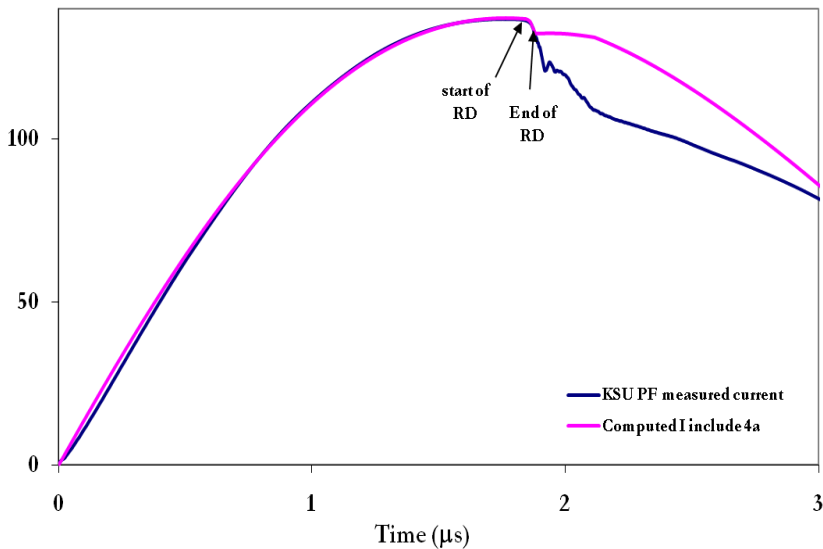
Radiation emission

Max. axial neutron yield	1.9×10^7 n/shot (6 mbar)	^3He detector
Max. radial neutron yield	1.05×10^7 n/shot (6 mbar)	^6LiI Detector
Neutron energy	2.45 MeV	Time of flight
Ion energy	Up to 130 keV	Faraday cup
Hard X ray average effective energy	59 ± 3 keV	Step filters and X-ray film

Lee model and high inductance devices

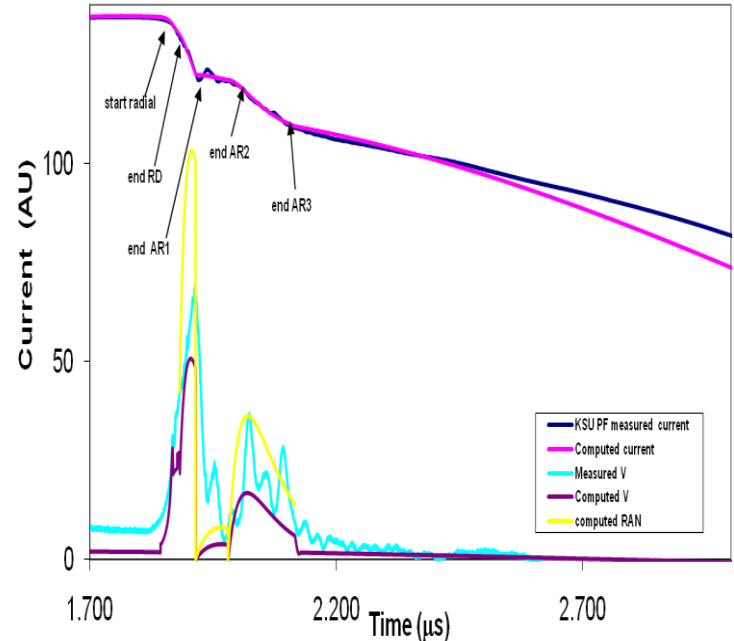
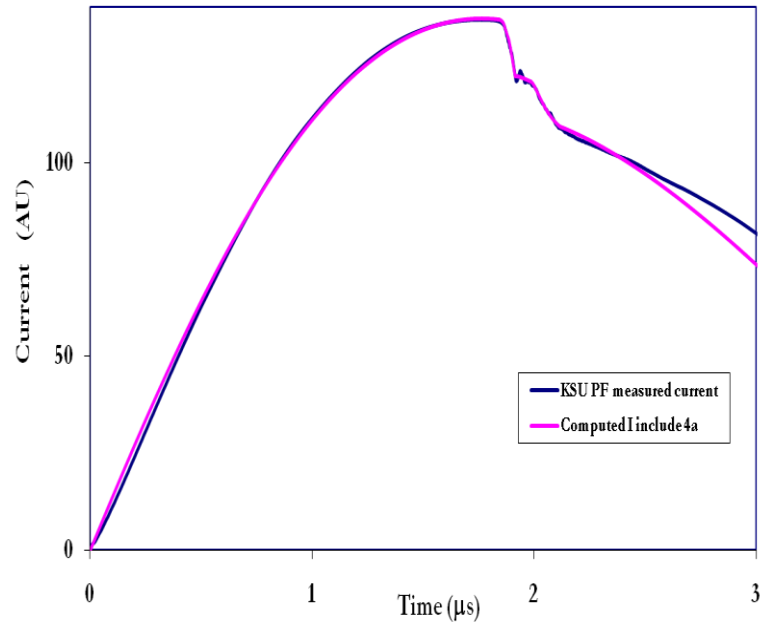


5-phase Lee model is found adequate for fitting all plasma focus with low static inductance L_0 , for example the PF1000 which trace shown in the figure



The KSU PF current trace has an extended dip (ED) beyond the regular dip (RD) computed by the 5-phase model.

- An extra phase was added by modeling an instability phase using fitted anomalous resistance terms.
- Devices was divided into T₁ (low inductance) and T₂ (high inductance).



Lee, S H Saw, A E Abdou & H Torreblanca, "Characterizing Plasma Focus Devices- Role of the Static Inductance-Instability Phase Fitted by Anomalous Resistances", J Fusion Energy, DOI 10.1007/s10894-010-9372-1

Explosive detection methods

- **Human and Biological based Methods**

Using trained dogs or manual inspections by well-trained people (Risky)

- **Trace-based Explosive Detections**

By detecting chemical trace of explosive material residues

- **Nonionizing Radiation-based Methods**

By using electromagnetic waves in different scales of frequencies like radiofrequency, Giga or Terahertz

Explosive detection methods

- **Nuclear-Based Explosive Detection Methods**

- **Neutron Interrogation Methods**

- High penetration power and not affected by electromagnetic waves.
- Interaction with the nuclei to produce characteristic γ -rays.
- Thermal and fast neutrons can be used in continuous or in pulsed form.

Explosive detection methods

Nuclear- based explosive detection methods

➤ X-ray based scanning methods:

- ❑ Conventional transmission X-ray radiography
- ❑ X-ray computed tomography (CT)
- ❑ Dual energy X-ray CT
- ❑ Scatter imaging (Back scattering Imaging system)

Nomenclature

- A target is an object under study that contains a sample.
- A sample is explosive if it is like a nitrogen-rich explosive.
- A sample is inert if it is not explosive.
- An interrogated sample is suspect if it is not clearly explosive or inert.
- **True positive (TP):** Correctly identified explosive.
- **True negative (TN):** Correctly identified inert.
- **False positive (FP):** Inert is identified as explosive.
- **False negative (FN):** Explosive identified as inert.

Signature- based radiation scanning (SBRS)

- Developed by Dunn at K-state.
- Active interrogation to detect explosives at standoff distances.
- The scattered or generated radiation from the target is collected by different detectors, producing signatures.
- A collection of different signatures for each unknown target is then compared to a template.
- The template is a collection of the same number of signatures for a known explosive-like sample.
- Template matching involves forming a Figure-of-Merit (FOM).

• **Figure of Merit**

$$\zeta = \frac{1}{N} \sum_{j=1}^J \alpha_j \frac{(\beta R_j - S_j)^2}{\beta^2 \sigma^2(R_j) + \sigma^2(S_j)}$$

R_j : Response vector , J is the number of signatures.

S_j : Template vector,

$\sigma^2(R_j), \sigma^2(S_j)$: Response and target variances, respectively.

α_j : Normalized positive weight factor ($\alpha_j = \frac{\omega_j}{\sum_{j=1}^J \omega_j}$)

β : A scaling factor that accounts for differences in the conditions.

**Standard
deviation**

$$\sigma(\zeta) = \frac{2}{N} \left[\sum_{j=1}^J \frac{(\alpha_j(\beta R_j - S_j))^2}{(\beta^2 \sigma^2(R_j) + \sigma^2(S_j))} \right]^{1/2}$$

Normalizing factor

$$N = \sum_{j=1}^J \alpha_j^2 \frac{S_{jl}^2}{\sigma^2(S_{jl})}$$

Cut-off value (f_0)

- For $(f - \sigma) > f_0$ -----> Inert (TN).
- For $(f + \sigma) < f_0$ -----> Explosive (TP).

Sensitivity & specificity

$$\text{Sensitivity} = \frac{\text{Number of true positive}}{\text{Total number of explosive samples used}}$$

$$\text{Specificity} = \frac{\text{Number of true negatives}}{\text{Total number of inert samples used}}$$

Experimental set-up

- X-ray Source (DPF).
- Targets: 5 gallons (9), 1 gallon (12), quart (11)

35% N fertilizer FertC	28% N fertilizer FertD	50/50 Mixture FertMix	Ammonium nitrate
Chalk	Rubber Mulch	Polyethylene	Aluminum
Sugar	Graphite	Sand	

- X-ray detectors.

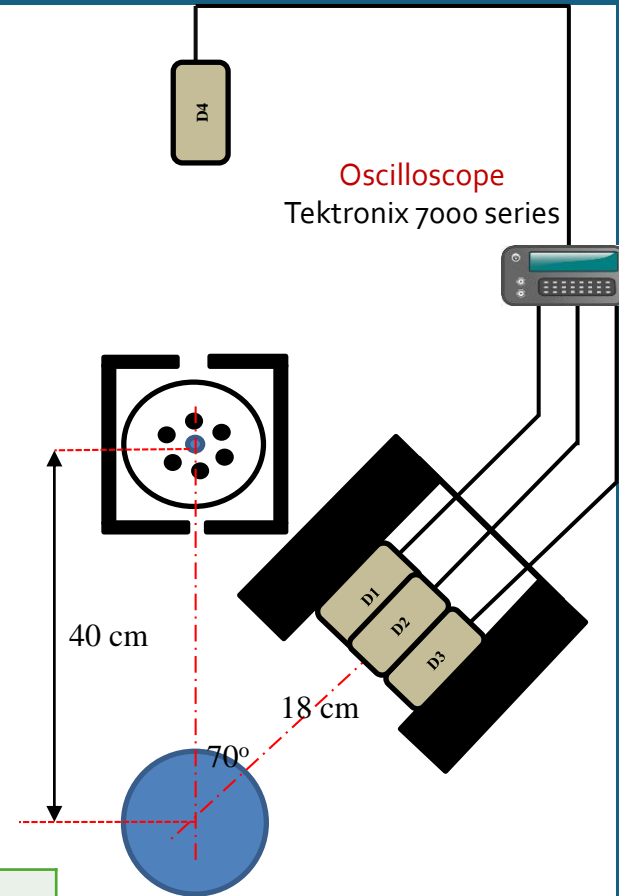
- A Canberra, 3x3 in., NaI(Tl), model 3M3/3-X.
- BC-418 plastic scintillator, 2 × 1 in.
HAMAMATSU PMT, model H7195.

D1: Bare Plastic scintillator

D2: Filtered NaI(Tl) scintillator

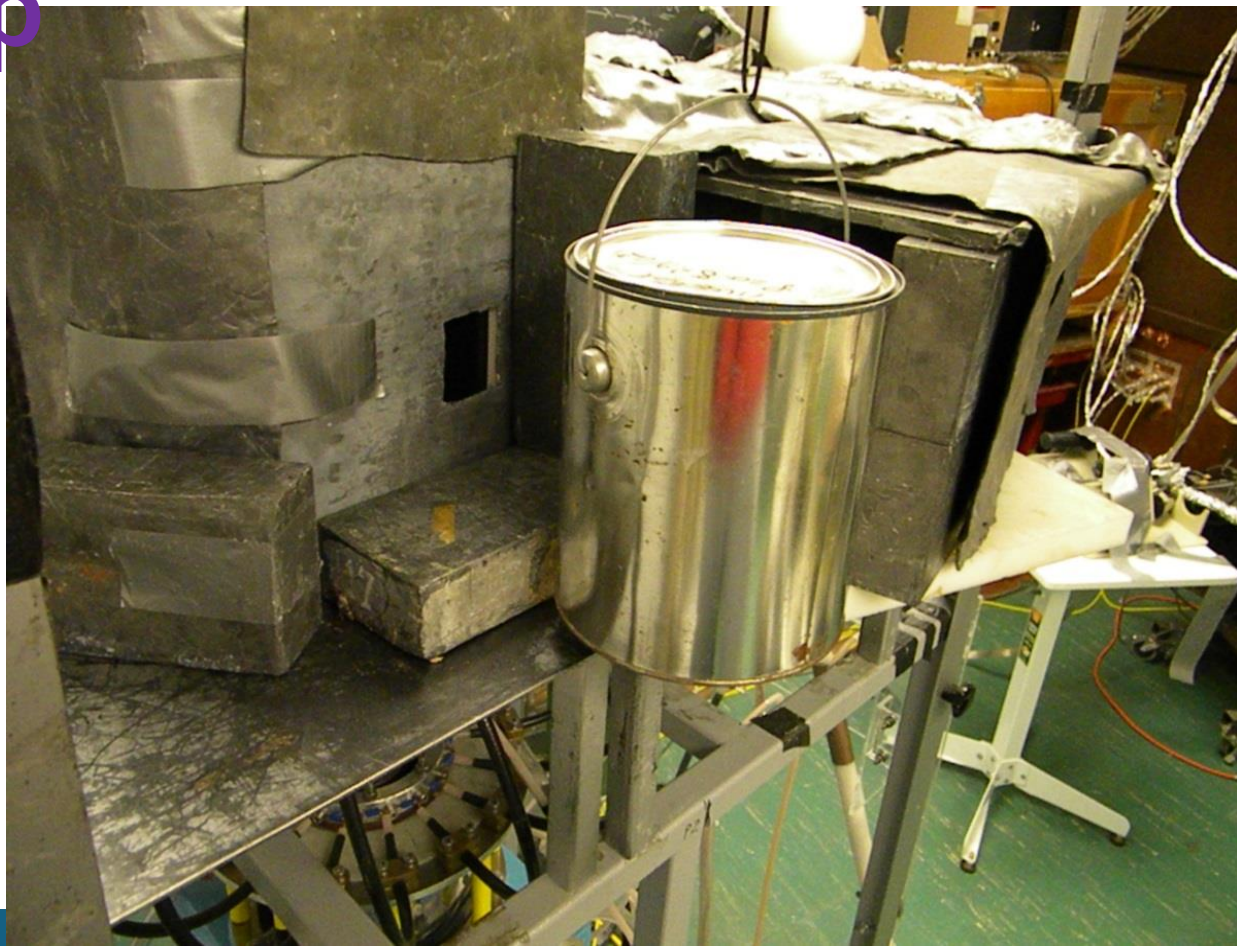
D3: Bare NaI(Tl) scintillator

D4: Bare NaI(Tl) scintillator

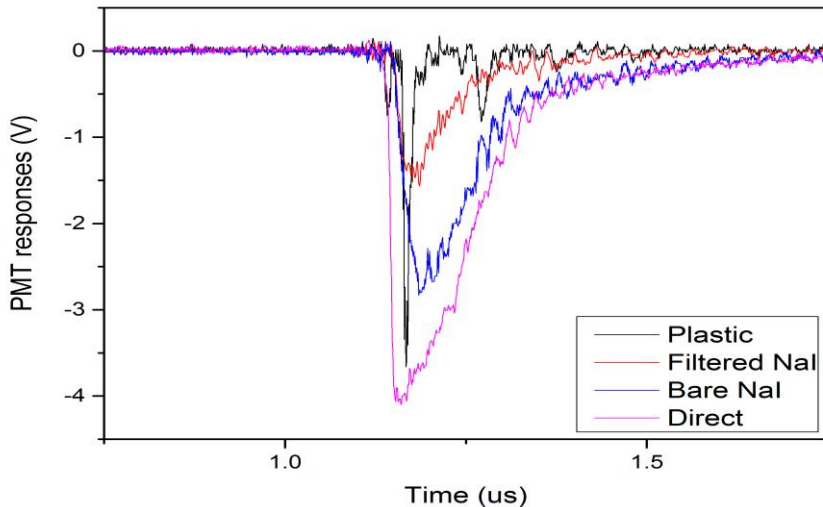


Experimental set-

up

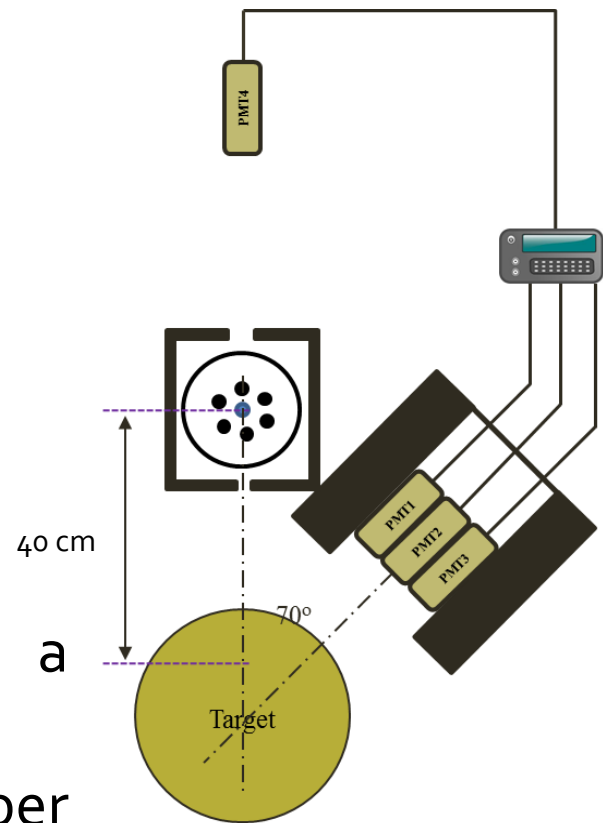


Experimental work



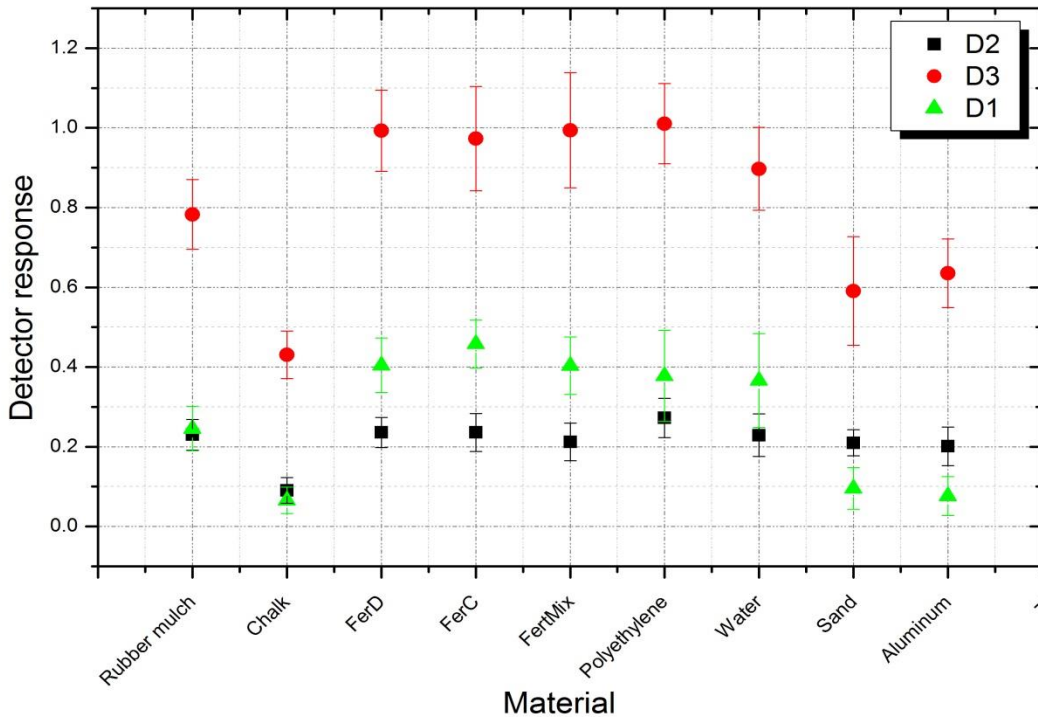
Response calculations

- Each curve is integrated to give a number
- This number is divided by the number obtained for the direct detector
- Average of 10 shots



Detector responses

Detectors' responses for 5-gallon cans.



D1: Bare Plastic scintillator.

D2: Filtered NaI(Tl) scintillator

D3: Bare NaI(Tl) scintillator.

Figure of merit (FOM)

5-gallon samples

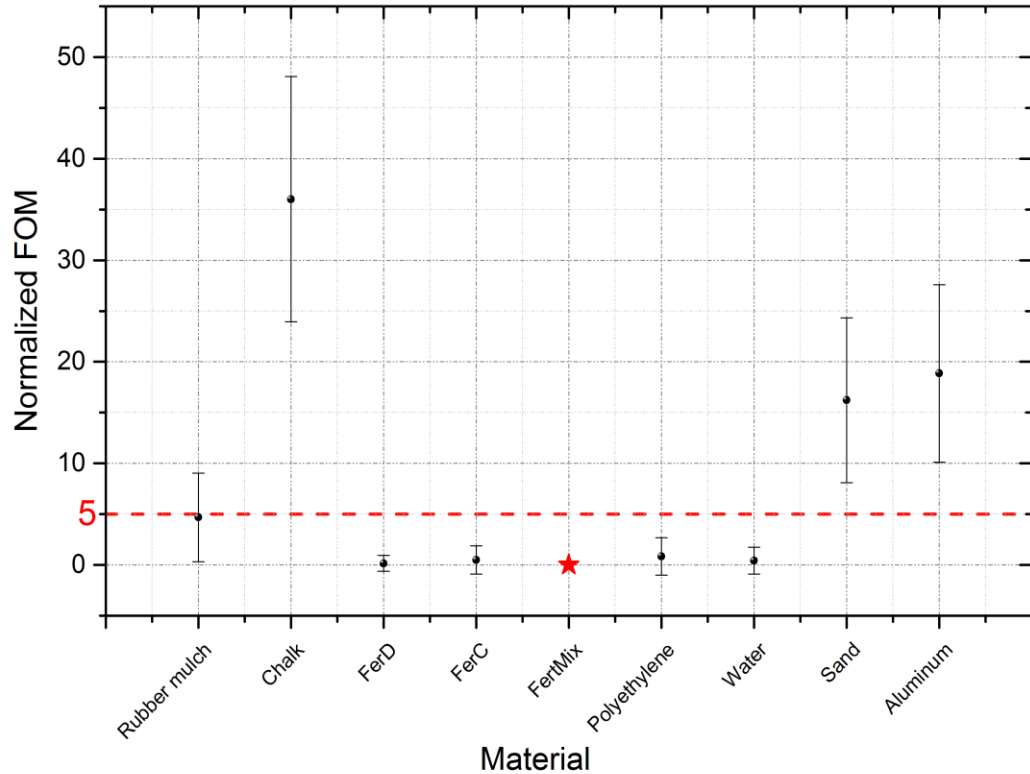


Figure of merit (FOM)

1-gallon samples

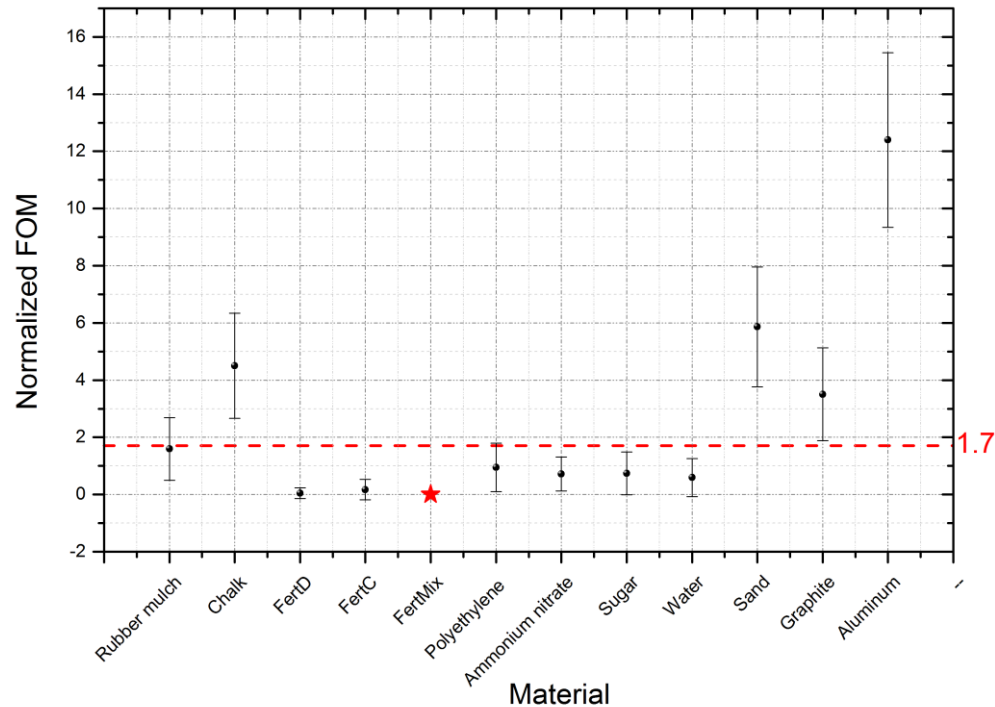
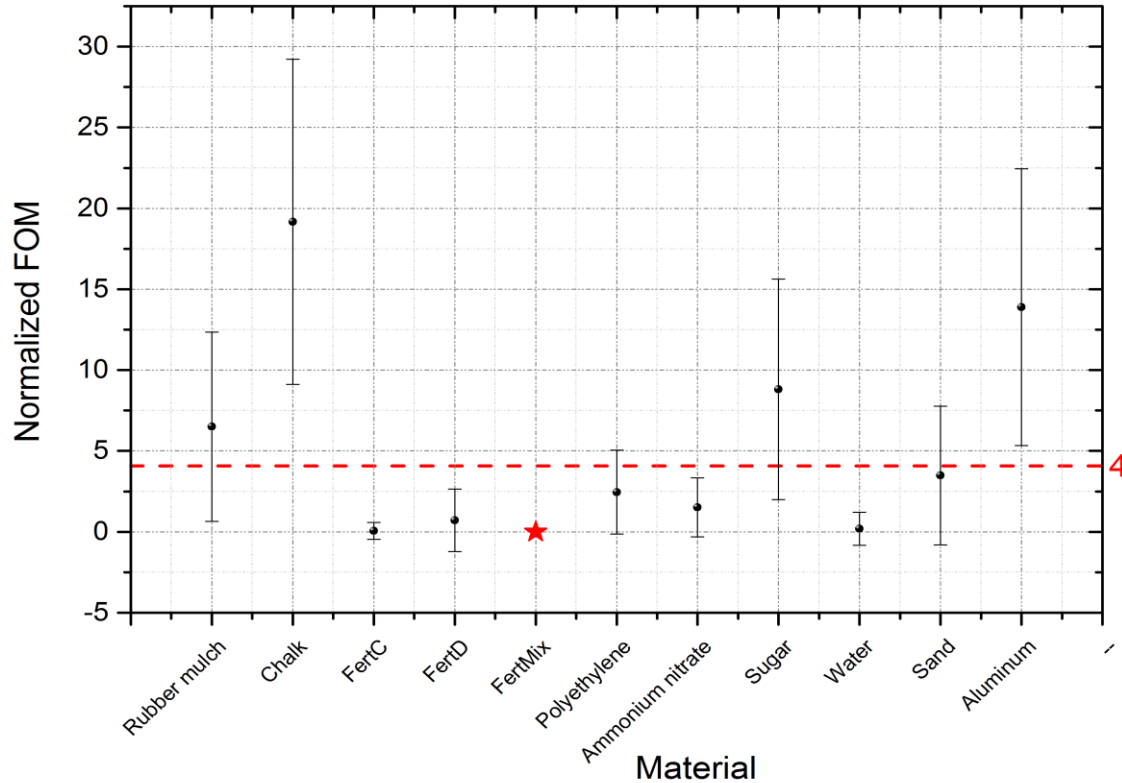


Figure of merit (FOM)

Quart samples

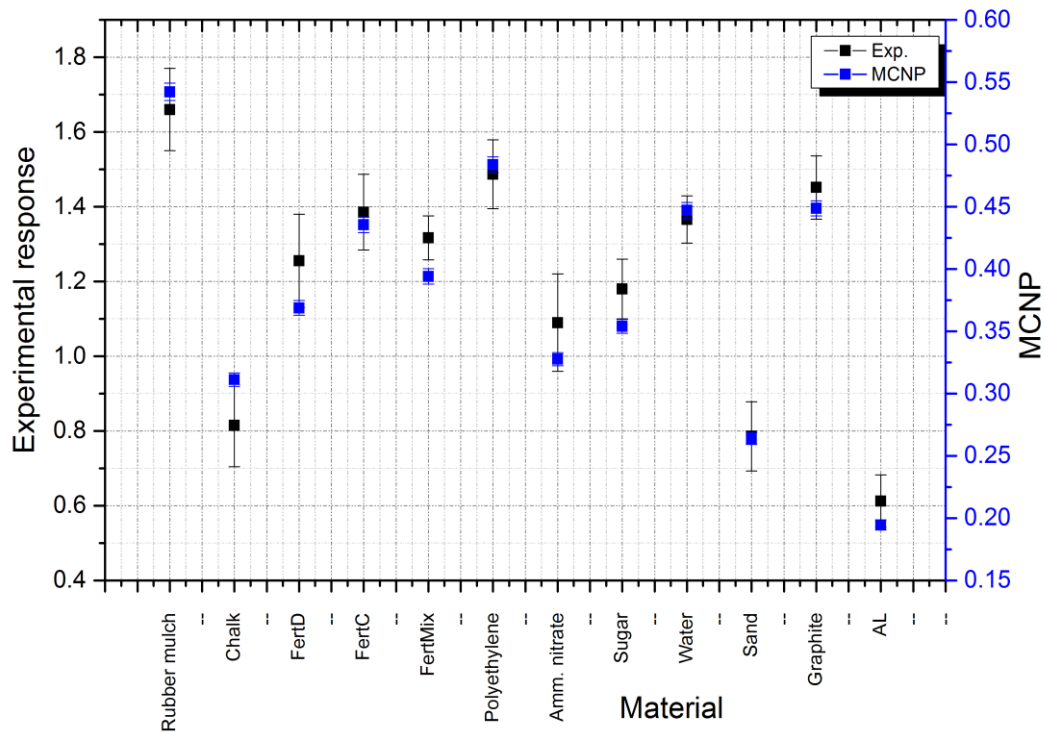


	5-gallons	1-gallon	Quart
Total # samples	8	11	10
Inert	6	8	7
Explosive-like	2	3	3
True (+ve)	2	3	3
True (-ve)	3	4	2
False (+ve)	2	2	1
False (-ve)	0	0	0
Suspect	1	2	4
Sensitivity%	100	100	100
Specificity%	50	50	28.6

Summary of experimental results

Comparison between experimental and simulation response for 1-gallon samples

- Hard to bring real explosives to the lab.
- More samples can be investigated using real explosives.
- Reasonable agreement between experimental and simulated detector responses.



Outline

- Introduction to dense plasma focus, construction and dynamics.
- KSU-DPF specifications and characterization.
- X-ray emission characteristics of the KSU-DPF.
- Introduction to explosive detection methods.
- Signature- based radiation scanning (SBRS).
- Experimental work for explosive detection.
- Simulation work.
- Conclusions.

Simulation

- MCNP-5: General purpose code used to simulate coupled neutron, photon and electron transport.

Cell card

- Cell, material number, density and importance to both neutrons and photons

Surface card

- Surfaces used to form the geometry

Data specification card

- Source type, the output type (tally), material specification, cross section library in addition to any other variance reduction technique

Simulation

A: Source.

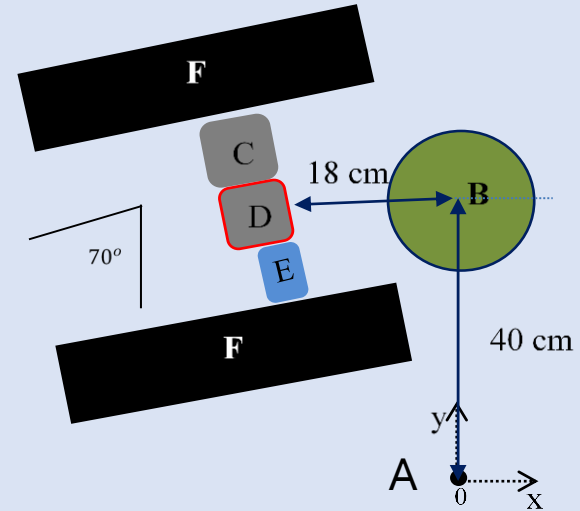
B: Target material 1-gallon.

C: Bare NaI(Tl).

D: Filtered NaI(Tl).

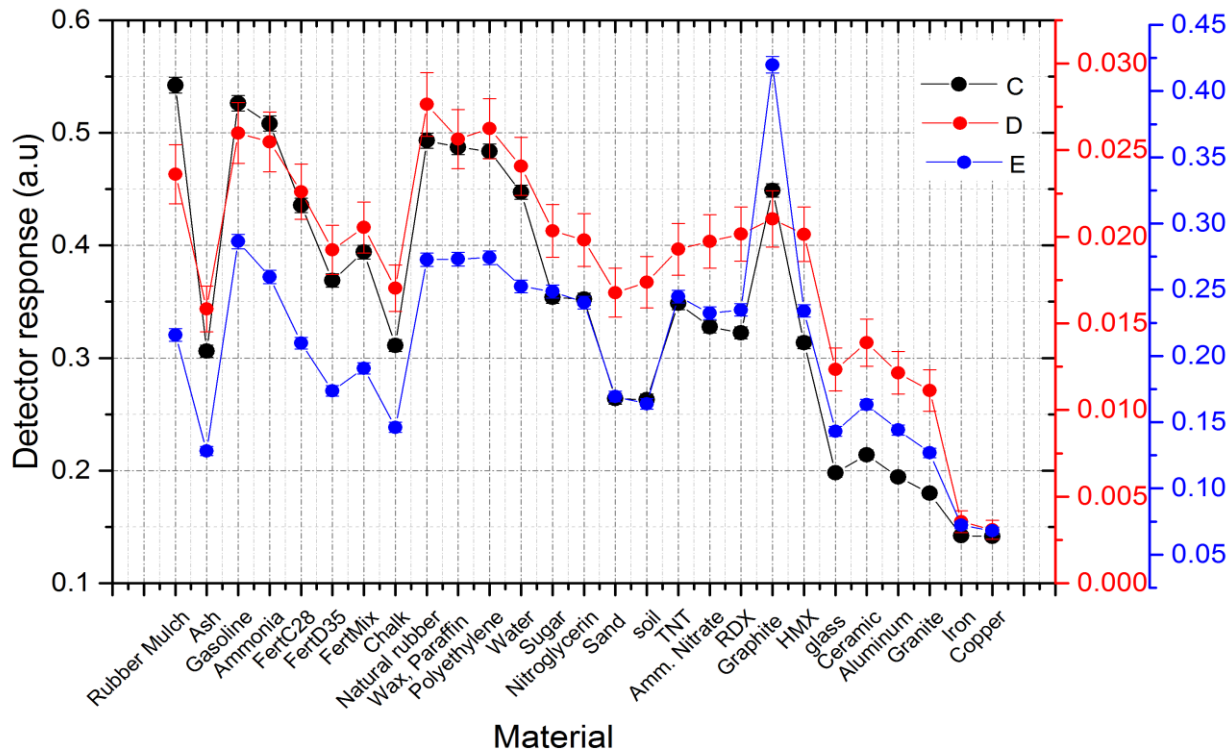
E: Bare plastic scintillator.

F: Lead shielding.

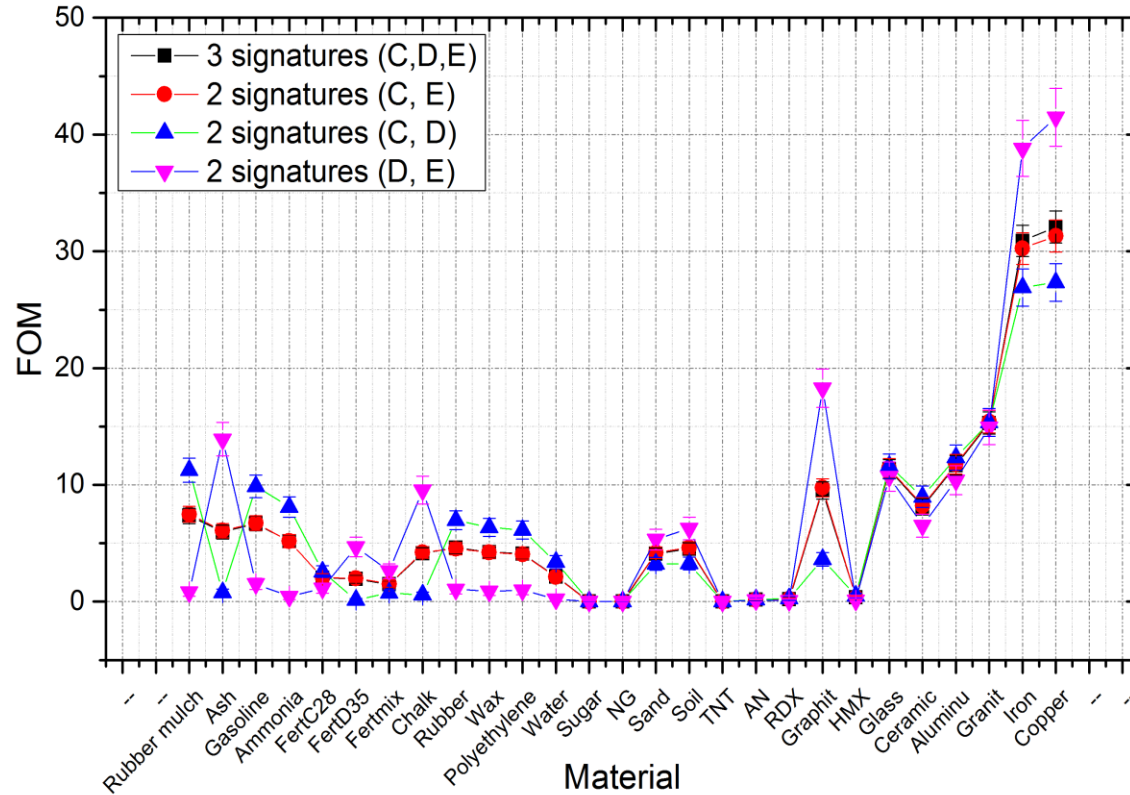


Simulation

1	Rubber mulch	15	Chalk
2	Ash	16	Natural rubber
3	Gasoline	17	Wax
4	Ammonia	18	Polyethylene
5	FertC	19	Water
6	FertD	20	Sugar
7	FertMix	21	Nitroglycerin
8	Sand	22	Glass
9	Soil	23	Ceramic
10	TNT	24	Aluminum
11	Ammonium nitrate	25	Granite
12	RDX	26	Iron
13	Graphite	27	copper

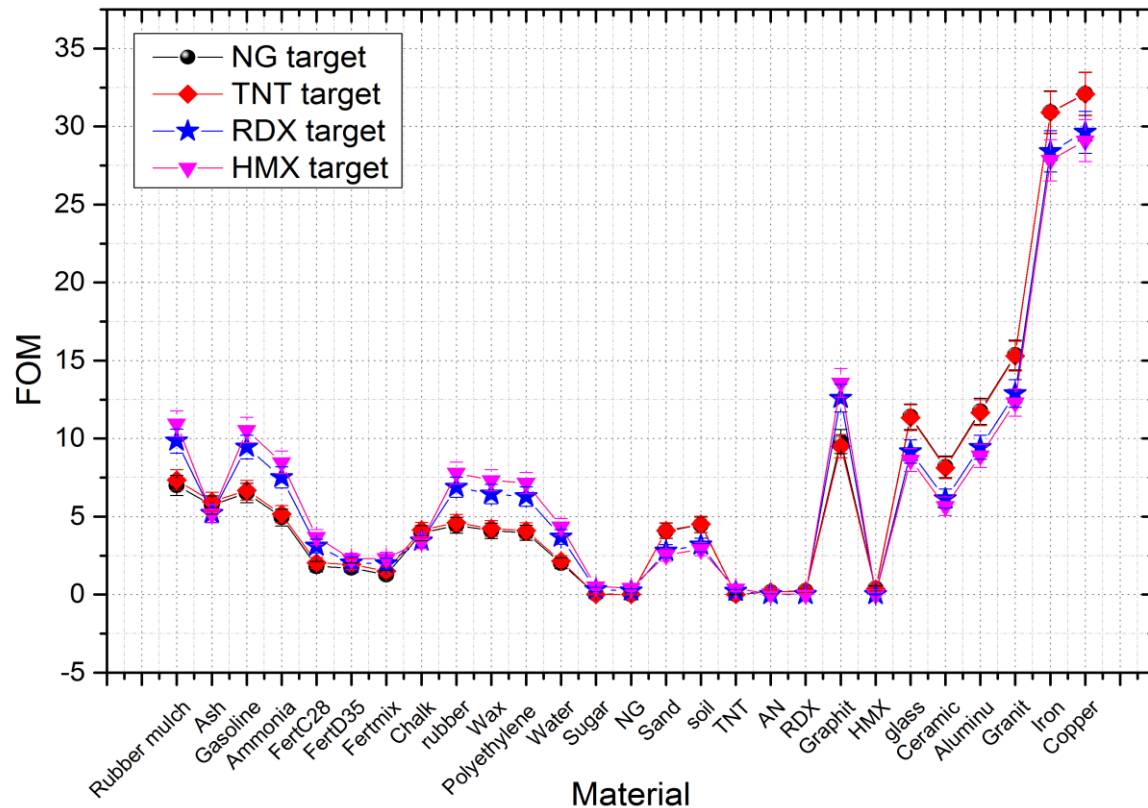


Simulation



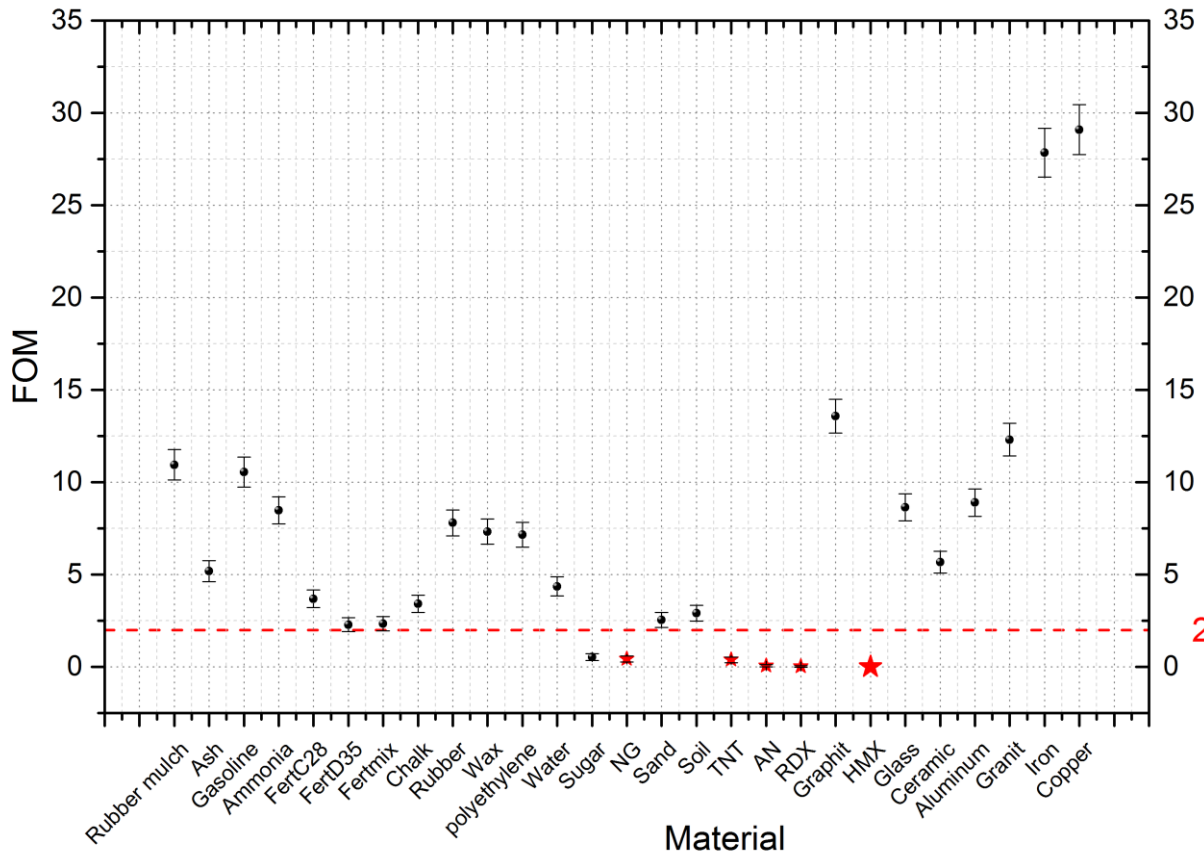
FOM of 3 responses
vs. different
combinations of 2
responses using
(TNT template)

Simulation



Comparison between the FOM for 3 responses using different templates.

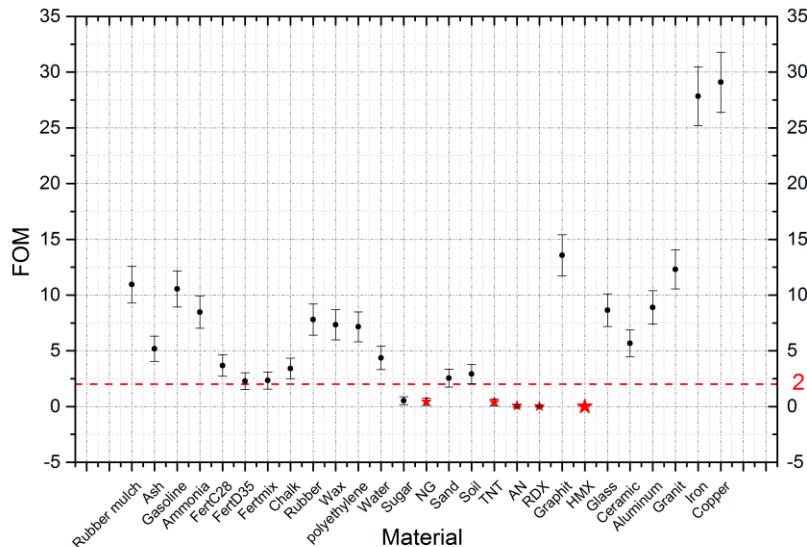
Simulation



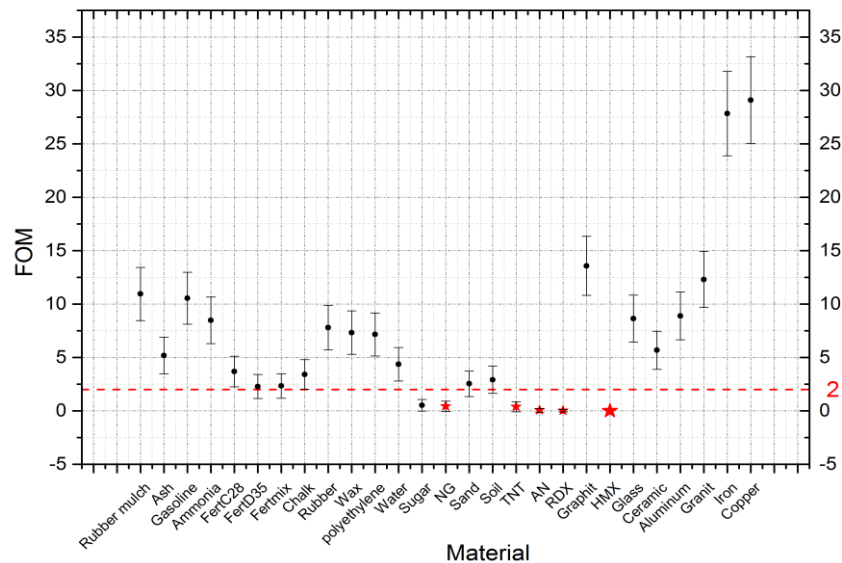
FOM for HMX
template using 1σ
(68% confidence)

2

Simulation



FOM for HMX template using
 2σ (95% confidence)



FOM for HMX template using
 3σ (99% confidence)

A Summary of simulation results for KSU-DPF

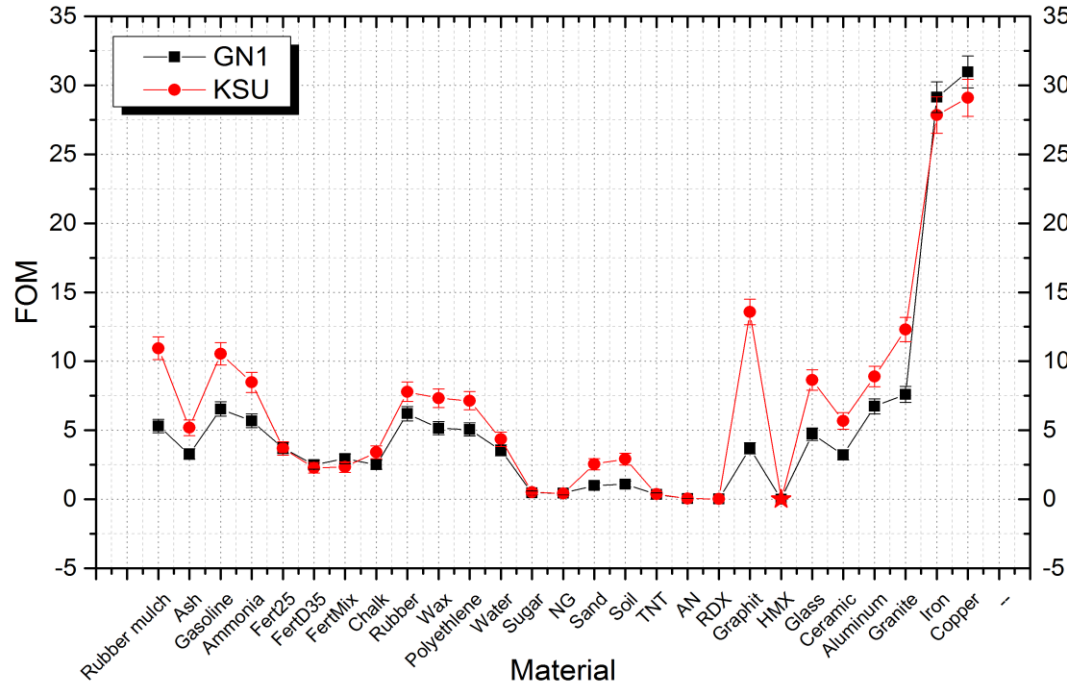
	1σ (68% confidence)	2σ (95% confidence)	3σ (99% confidence)
Inert samples	22	22	22
Explosives	5	5	5
True positives	5	5	5
True negatives	18	17	15
False positives	1	1	1
False negatives	0	0	0
Suspect	3	4	6
Sensitivity %	100	100	100
Specificity %	81.8	77.3	68.2

GN₁ Simulation

- 4.7 kJ device when charged at 30 kV and HXR of ~ 100 keV

	1σ (68% confidence)	2σ (95% confidence)	3σ (99% confidence)
Inert samples	22	22	22
Explosives	5	5	5
True positives	5	5	5
True negatives	17	16	14
False positives	3	3	3
False negatives	0	0	0
Suspect	2	3	5
Sensitivity %	100	100	100
Specificity %	77.3	72.7	63.6

GN₁ Simulation



Comparison between the FOM for simulation for both KSU-DPF and GN₁

Conclusion

- The KSU-DPF was commissioned to be used as a multi-radiation source; used for radiography and explosive detection.
- The device has an inductance of 91 ± 2 nH and resistance 13 ± 3 m Ω and can store energy up to 10 kJ.
- Experiments showed that the device emits around 1.9×10^7 n/pulse of 2.45 MeV neutrons at an optimum pressure of 6 mbar of deuterium.
- The HXR average effective energy was measured to be 59 ± 3 and the spectrum ranges from 20 up to 120 MeV with a most probable value of 53 MeV.

Conclusion

- DPF allows rapid interrogation because of the short pulse time; good for high-volume testing.
- We tested simple targets with uniform contents.
- Experimental results with 100% sensitivity and reasonable specificity (50% for gallon and larger samples) were obtained.
- Simulations obtained similar results with real explosives and more inert materials with 100% sensitivity and 82, 77 and 68 specificity for 68, 95 and 99% of confidence.

